

IMPEDANCE AND CONDUCTIVITY ANALYSIS OF Li_2SiO_3 CERAMIC

ABHIJIT PRASAD^{*}, AMITABHA BASU AND MANOJ KUMAR MAHATA
Department of Applied Physics, Indian School of Mines, Dhanbad-826004, India

Lithium metasilicate (Li_2SiO_3) ceramic was prepared via solid-state reaction technique. The formation of the compound in an orthorhombic crystal structure was confirmed by an X-ray diffraction (XRD) technique. Surface morphology of the compound was studied by field emission scanning electron microscopy (FE-SEM). Detailed studies on the electrical behavior (complex impedance [Z^*], electrical conductivity and relaxation mechanism) of the Li_2SiO_3 ceramic have been carried out at various temperatures. The Nyquist plots suggest that the grains and grain boundaries are responsible in the conduction mechanism of the material at high temperature. The frequency dependent conductivity and dielectric relaxation of Li_2SiO_3 ceramic are investigated over a frequency range from 100 Hz to 5 MHz and in a temperature range from 35 °C to 350 °C by using alternating current impedance spectroscopy. The conductivity isotherms show a transition from frequency independent dc region to dispersive region where the conductivity continuously increases with the increasing frequencies.

(Received July 15, 2011, accepted August 17, 2011)

Keywords: Ceramics; Grain boundaries; Impedance properties; Sintering

1. Introduction

Lithium ceramics are of research interest because of their technological applications. Thus, for example, there has been research in recent years on their application as electronic devices, as CO_2 captors and as breeder materials for nuclear fusion reactors, in addition to other more well-known applications such as in batteries and in low thermal expansion glass ceramics used in ceramic hobs [1–10]. Various properties of Lithium silicate ceramics such as dielectric, conductivity and other properties depend on the composition and microstructure. In this paper, we present a systematic study of Lithium metasilicate (Li_2SiO_3) ceramic prepared by solid state reaction technique and the influence of temperature and frequency on impedance properties.

2. Experimental

2.1. Material preparation

Lithium metasilicate (Li_2SiO_3) ceramic was prepared using a high-temperature solid-state reaction technique. Li_2CO_3 and SiO_2 of analytical grade were thoroughly mixed in agate mortar for 2 h, including wet mixing in acetone media for 1 h. The mixture was then calcined at 900 °C for 4 h. The calcined powder was then cold pressed into cylindrical pellets of 12 mm diameter and 2 - 3 mm of thickness at a pressure of 80 MPa using a hydraulic press. PVA (poly vinyl alcohol) was used as a binder for preparing pellets. These pellets were then sintered with optimized temperature and time (900 °C, 2 h) in an air atmosphere.

^{*}Corresponding author: abhijit_133@rediffmail.com

2.2. Material characterization

The formation of the single phase compound was confirmed by X-ray diffraction (XRD) in a wide range of Bragg angles 2θ ($10^\circ \leq 2\theta \leq 90^\circ$) with Co radiation (1.78897 \AA). The surface morphology was recorded using field emission scanning electron microscope. The electrical parameters were measured using an impedance analyzer (HIOKI LCR HI Tester, Model: 3532) as a function of temperature over a wide range of frequencies (100 Hz – 5 MHz) after drying the silver coated sample at 150°C for 2 h.

3. Results and discussion

3.1. Structural

The XRD pattern of the sintered sample is shown in Fig. 1. Detailed analysis of the pattern exhibits the formation of new compound in orthorhombic crystal system with lattice parameters: $a=9.396 \text{ \AA}$, $b=5.396 \text{ \AA}$, $c=4.661 \text{ \AA}$, which is in well agreement with the structure given in JCPDS file number 83-1517. The crystallite size (D) of the compound was determined using the broadening of a few XRD peaks using the Scherrer's equation [11], $D = 0.89\lambda / (\beta_{1/2} \cos \theta)$, where $\lambda = 1.78897 \text{ \AA}$ and $\beta_{1/2}$ is the peak width of the reflection at half intensity. The average crystallite size was found to be $\sim 30 \text{ nm}$. Other effects of the broadening were ignored.

Fig. 1 (inset) shows the field emission scanning electron micrograph of the sample at room temperature. The FESEM micrograph was taken on the fractured surface of the sample using scanning electron microscope. The highly distinctive, more or less uniform and compact grain distributions (with less voids) are observed. It shows the polycrystalline texture of the material. The average grain size was found to be $1 - 3 \text{ \mu m}$.

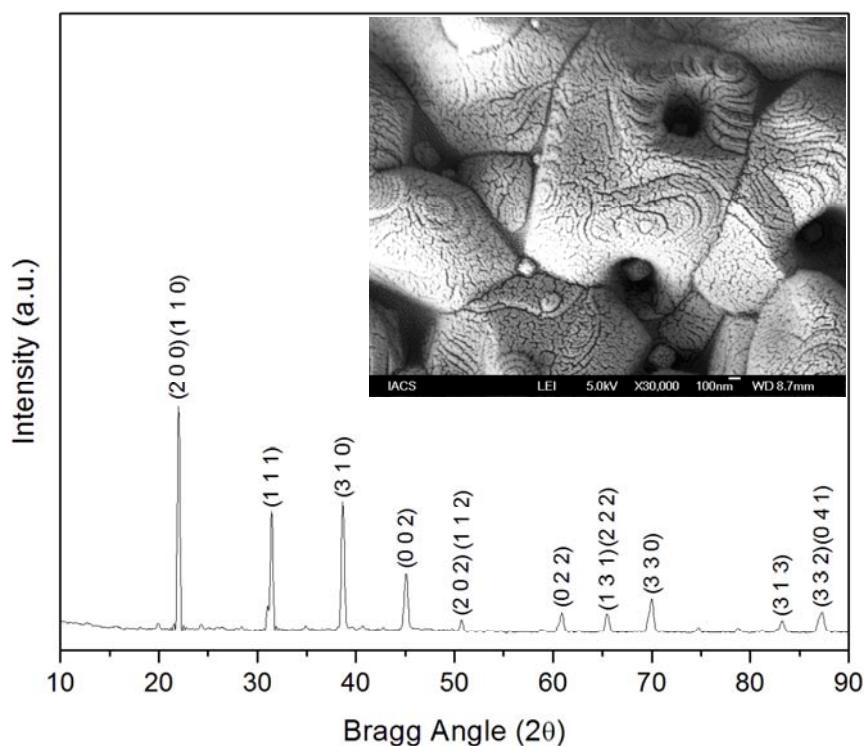


Fig. 1. Room temperature XRD pattern and FE-SEM micrograph (inset) of Li_2SiO_3 ceramic.

3.2. Impedance analysis

Fig. 2(a) exhibits the variation of real part of impedance (Z') with frequency at different temperature. The decrease in the magnitude of Z' with the increase in both frequency as well as temperature indicates the increase in a.c. conductivity. The values of Z' merge at higher frequency (≥ 25 kHz) which indicates the release of space charges. Fig. 2(b) represents the impedance loss spectrum (i.e. variation of imaginary part of impedance [Z''] with frequency). The nature of the pattern is characterized by (1) decreasing the height of the peaks with rising temperature (2) significant broadening of the peaks with the rising temperature and (3) marked asymmetry in the peak pattern. The curves show that the value of Z'' reaches maximum value of Z''_{\max} for temperature ≥ 250 °C.

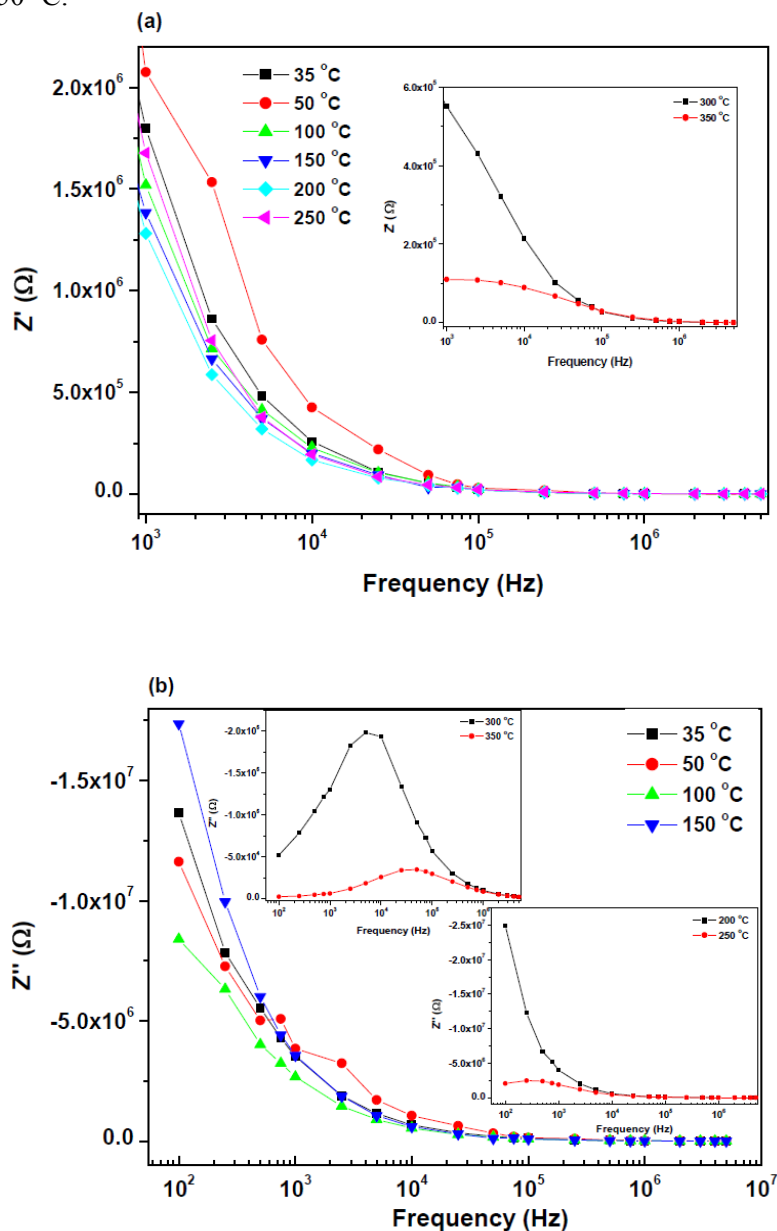


Fig. 2. Variation of (a) real part of impedance (Z') and (b) imaginary part of impedance (Z'') of Li_2SiO_3 ceramic as a function of frequency.

The relaxation time (τ) was calculated from the frequency maxima (f_{\max}) at Z''_{\max} . At the peak, the relaxation is defined by the condition:

$$\omega_m \tau_m = 2\pi f_{\max} \tau_m = 1$$

where, τ_m is the relaxation time and f_{\max} is the relaxation frequency. It is independent of the sample geometrical factors and depends basically on the intrinsic property of the material only. Relaxation time of the sample decreases with the increase in temperature (Table 1). This result suggests the presence of temperature-dependent electrical relaxation phenomenon in the material possibly due to migration of immobile species/defects.

Table 1: Relaxation time (τ), Bulk Resistance (R_b) and Relaxation Frequency (f_b) of Li_2SiO_3 ceramic.

Temperature ($^{\circ}\text{C}$)	Relaxation time (τ) (in ms)	Bulk Resistance (R_b) (in $\text{k}\Omega$)	Relaxation frequency (f_b) (in kHz)
250	5.831×10^{-1}	6967.33	0.4
300	2.915×10^{-2}	608.42	5
350	2.915×10^{-3}	114.64	50

The Nyquist diagram (Z'' vs. Z') obtained at different temperature over a wide range of frequencies (100 Hz - 5 MHz) has been displayed in the figure 3(a). The effect of temperature on the impedance parameter of the material becomes clearly visible with rising temperature. The straight lines with large slopes at lower temperature indicate the insulating behavior of the material. However, on increasing temperature, the slope of the lines decreases, and hence they bend towards Z' - axis by which semicircle could be formed. The intercept of the semicircle on the real axis is the bulk resistance (R_b) (given in Table 1) of the sample. The resistance is obtained from the intersection of the semicircle and the Z' axis. It is clear from the figure that the resistance decreases on increasing temperature. At much higher temperature (i.e. at 350 $^{\circ}\text{C}$); It was possible to trace two semicircles (i.e. figure inset). The appearance of two semicircles suggests the presence of both bulk as well as grain boundary effects in the polycrystalline sample. Each semicircle is a representative of RC circuit that corresponds to individual component of the material (Fig. 3(b) [inset]).

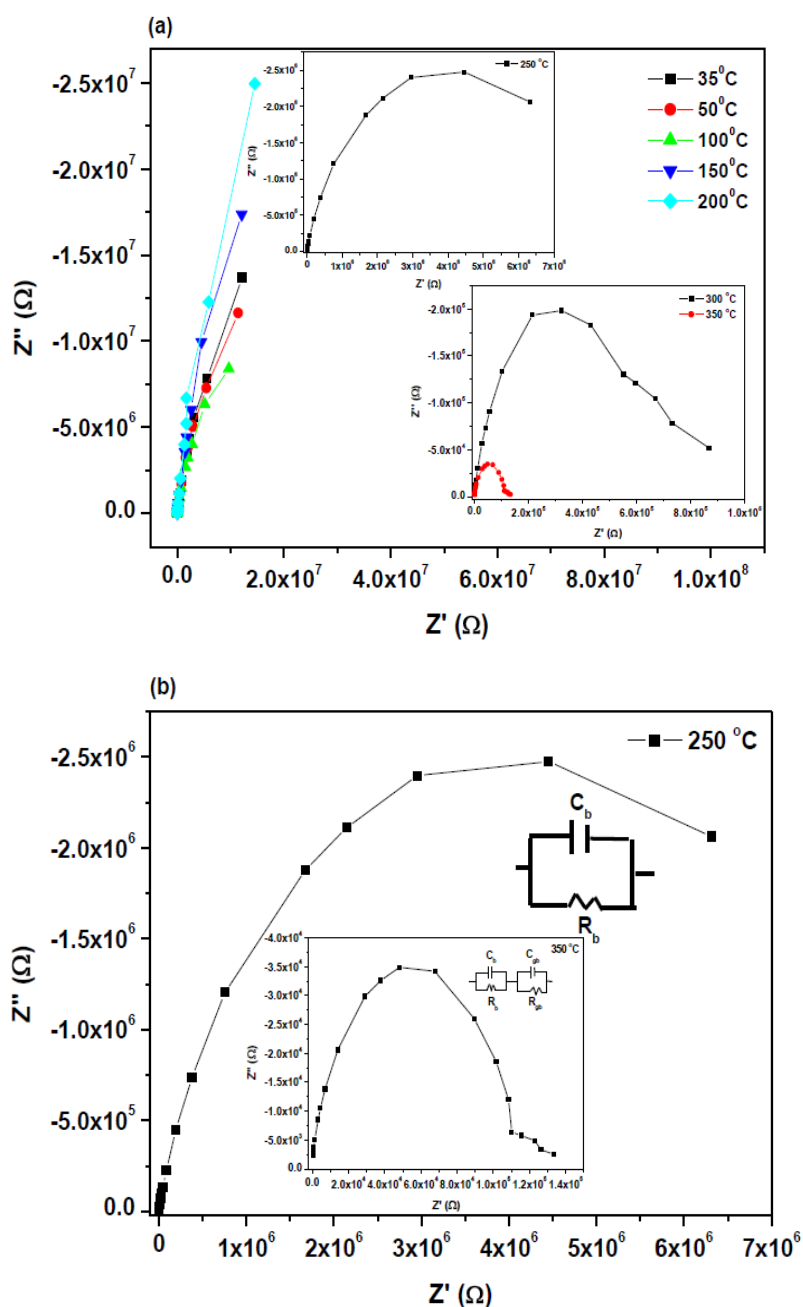


Fig. 3. (a) Nyquist plots of Li_2SiO_3 ceramic at different temperatures (b) Nyquist plots of Li_2SiO_3 ceramic with equivalent circuit (inset)

3.2. ac conductivity analysis

The electrical conductivity (ac) of the material has been investigated at different temperatures over a wide range of frequency. The ac electrical conductivity of the sample was calculated from the conductivity relation $\sigma = \omega \epsilon_0 \epsilon \tan \delta$ where ϵ_0 is the vacuum dielectric permittivity and ω is the angular frequency. Fig. 4 shows the frequency dependence of ac conductivity, $\sigma(\omega)$ at various temperatures. It is evident from the figure that at low frequencies, conductivity shows frequency independent nature of the sample which gives rise to dc conductivity. However, at the higher frequencies, σ exhibits frequency dispersion. At higher temperatures (i.e. $\geq 300^\circ\text{C}$), σ exhibits frequency dispersion in low as well as in high frequency

regions. The temperature, at which grain resistance dominates over grain boundary resistance, is marked by a change in slope of ac conductivity with frequency. The frequency at which the change of slope takes place is known as the hopping frequency. The a.c. conductivity of the sample increases with the increase of temperature.

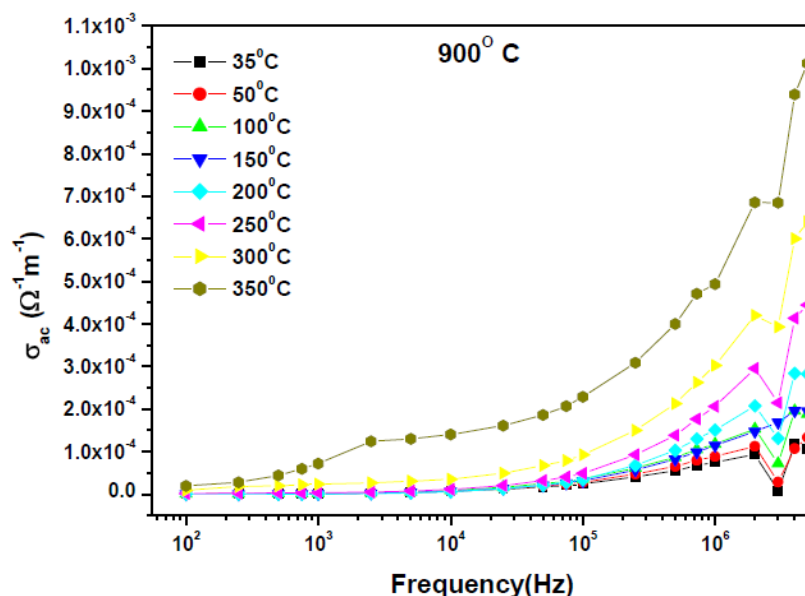


Fig. 4. Frequency dependence of a.c. conductivity (σ_{ac}) at various temperatures for Li_2SiO_3 ceramic sintered at 900°C for 2 h.

4. Conclusions

The Li_2SiO_3 ceramic was prepared by a solid-state reaction technique. X-ray structural study reveals an orthorhombic crystal structure of the material. The surface morphology of the compound is studied through FE-SEM, which shows the uniform distribution of well compacted grains throughout the sample. The electrical parameters such as the real and imaginary parts of impedance and ac electrical conductivity as a function of frequency at different temperature have been studied through complex impedance spectroscopy. Nyquist plots show the presence of bulk and grain boundary effects in the system. The nature of variation of (ac) conductivity with temperature exhibits the NTCR behavior of the sample like that of a semiconductor.

References

- [1] C. A. Vincent, *Solid State Ionics* **134**, 159–167 (2000).
- [2] C.-H. Lu and L. Wei-Cheng, *J. Mater. Chem.* **10**, 1403–1407 (2000).
- [3] M. Broussely, F. Pertion, P. Biensan, *J. Power Sources* **54**, 109–114 (1995).
- [4] V. Subramanian, C. L. Chen, H. S. Chou, G. T. K. Fey, *J. Mater. Chem.* **11**, 3348–3353 (2001).
- [5] X. Yang, W. Tang, H. Kanoh, K. Ooi, *J. Mater. Chem.* **9**, 2683–2690 (1999).
- [6] H. Kudo, K. Okuno, S. O'Hira, *J. Nucl. Mater.* **155–157**, 524–528 (1988).
- [7] H. Pfeiffer, P. Bosch, S. Bulbulian, *J. Mater. Chem.* **10**, 1255–1258 (2000).
- [8] H. Pfeiffer, P. Bosch, *Chem. of Mater.* **17**, 1704–1710 (2005).
- [9] H. A. Mosqueda, C. Vazquez, P. Bosch, H. Pfeiffer, *Chem. of Mater.* **18**, 2307–2310 (2006).
- [10] H. Pfeiffer, C. Vazquez, V. H. Lara, P. Bosch, *Chem. of Mater.* **19**, 922–926 (2007).
- [11] P. Scherrer, *Göttinger Nachrichten.* **2**, 98 (1918).